Monitoring tropical cyclone evolution over the NW Pacific with Aqua AMSR-E and Envisat ASAR

Leonid M. Mitnik, Maia L. Mitnik, Irina A. Gurvich

V.I. Il'ichev Pacific Oceanological Institute FEB RAS, 690041 Vladivostok, Russia – (mitnik, -maia, -gurvich)@poi.dvo.ru

Abstract - The quantitative monitoring of tropical cyclones (TCs) over the ocean is one of the most important applications for satellite passive and active microwave sensors. Aqua AMSR-E microwave measurements can contribute quantitative ocean surface and atmospheric information in cloudy and rainy conditions. Envisat advanced SAR and QuikSCAT SeaWinds scatterometer can also contribute information on sea surface wind and precipitation within a swath width of 405 and 1445 km with a resolution of 150 x 150 m and 12.5 x 12.5 km, respectively. The Northwest Pacific typhoons Aere and Songda were analyzed with AMSR-E and SeaWinds data taken during their most active stage. The developed tropical algorithms were applied to the measured brightness temperatures to retrieve total atmospheric water vapor content, total cloud liquid water content, wind speed, and delineate the precipitation zones. Envisat ASAR images of Aere and Songda revealed the fine features in surface wind and precipitation distributions.

Keywords: Tropical cyclone, Aqua AMSR-E, Envisat ASAR, water vapor, cloud liquid water content, retrieval algorithms.

1. INTRODUCTION

The availability of satellite SeaWinds scatterometer since 1999 and AMSR-E microwave radiometer since 2002 has provided an enormous amount of wide swath (1440-1800 km) but low-resolution (5-25 km) data capable of quantitative monitoring a variety of the marine weather systems. Their joint analysis with Envisat advanced synthetic aperture radar (ASAR) operating in a wide swath regime (405 km) allows to combine a synoptic view of a system with detection of the fine details of sea surface wind and heavy precipitation patterns. Advantages of this approach was realized earlier on Kosmos-1500 (launched in 1983), Kosmos-1776 (in 1986), as well as on the Okean series satellites which carried out a set of sensors consisting of a 3-cm vertically polarized real aperture radar (RAR), a 0.8 cm horizontally polarized side-scanning microwave radiometer and four-channel visible imaging system. RAR swath width was ≈ 460 km and the spatial resolution was 2.1-2.8 km (in flight direction) by 0.8-3 km (normal to flight) (Kalmykov, 1996).

The unique capability of this series, the simultaneous acquisition of overlapping images by three different sensors at three different wavelengths, enabled an improved interpretation of measurements and a reduction in errors of retrieved parameters since active and passive sensors, being sensitive to different physical properties of the ocean-atmosphere system, provide results that complement each other. It was shown, in particular, for tropical storm Agnes (Mitnik et al., 1990). Then such a capability was employed by combination of Okean RAR images with the SSM/I data taken over the Northwest Pacific typhoons. Individual rain cells in the typhoon rain bands and the wind field features were clearly identified on RAR images whereas a time set of SSM/I data allowed to trace evolution of total water vapour content, total cloud liquid water content and precipitation in the typhoon area (Mitnik et al., 1997, 1998, 2002).

The combination of wide swath SAR images taken by RADARSAT and Envisat with data acquired by other remote sensors such as SeaWinds scatterometer and AMSR/AMSR-E microwave radiometer as well as sensors operating in visible and infrared spectral bands is a technique that has attracted increasing scientific interest over the last years since high resolution data provided SAR revealed the new features important for better understanding of typhoon's evolution (Friedman and Li, 2000; Katsaros et al., 2002; Vachon et al., 2001). The paper presents examples of tropical cyclone's study with the using of two active sensors (SeaWinds and ASAR) and one passive microwave sensor (AMSR-E).

2. DATA SETS AND BACKGROUND

2.1 2004 typhoon season

The 2004 Northwest Pacific season was characterized by a reach variety of tropical cyclones (TCs). 29 TCs was formed in the area from 5 April till 22 December. Their lifetime and strength varied from 6 hours (tropical storm Merbok with minimum pressure P_{min} = 1000 mb and maximum wind speed W_{max} = 17 m/s) till 11.8 days (super typhoon Chaba, P_{min} = 910 mb, W_{max} = 57 m/s). 21 TC reached typhoon stage. Envisat ASAR images in a wide swath regime at a resolution of 150 x 150 m were obtained for Aere (2 images) и Songda (4 images). These typhoons were chosen for detailed study.

2.2 Instruments

AMSR-E aboard the EOS AQUA platform is conically scanning passive microwave radiometer sensing microwave radiation at 12 channels and 6 frequencies ranging from 6.9 to 89.0 GHz. Brightness temperatures $T_B(\nu)$ with horizontal (H) and vertical (V) polarization are measured separately at each frequency ν. The scanning angle of 47.4° results in an Earth incidence angle of 55.0°. The spatial resolutions of the 6 frequencies are from 74 x 43 km for 6.9 GHz channels to 6 x 4 km for 89.0 GHz channels (Parkinson, 2003).

ASAR aboard the Envisat satellite operates at C-band at several regimes. Wide Swath Mode gives a 400 km by 400 km wide swath image with VV or HH polarisation using five predetermined overlapping antenna beams which cover the wide swath. Spatial resolution is approximately 150 x 150 m. Probability to catch typhoon and especially its eye is low since time operation is limited by 30 min for each orbit.

SeaWinds scatterometer aboard QuikSCAT satellite operates at frequency of 13.4 GHz. 1800-km swath during each orbit provides ≈ 90% coverage of Earth's oceans every day. An

accuracy of wind speed/direction measurements is 2 (m/s)/20 deg at W = 3-20 m/s. The antenna elliptical footprint is 30 km x 40 km, but with range signal processing of the chirped transmitted pulse, the sigma-0 is resolved into 4 km x 25 km "slices". Using the sigma-0 slices, it is possible to produce 12.5 x 12.5 km wind vector cells.

3. TYPHOONS

3.1 Typhoon Aere

Aere originally formed as a tropical depression on the 19th of August at 12.7°N, 136.4°E. It shifted northwestward and deepened. Aere reached maximum intensity at 03 UTC on 24 August at P_{min} = 955 mb and wind speed near the center was 41 m/s. The measurements carried out by microwave sensors such as TRMM TMI at 01:54 and 08:25 UTC, Aqua AMSR-E at 04:40 UTC, QuikSCAT SeaWinds at 09:32 UTC as well as by visible and infrared sensors such as Aqua MODIS, NOAA AVHRR and GOES-9 allowed to visualize structure of cloudiness, precipitation, cloud liquid water content and total water vapor content. As we see in Fig. 1a, large cold eye the diameter of 80 km, eye wall and spiral rain bands of Aere are clearly manifested themselves on the AMSR-E T_B(36H) image due to high brightness contrasts. The eye is cold: it is characterized by low T_B(36H) $\approx$ 200 K due to the absence of clouds. Eye wall, a circle the width of 20-30 km, is hot: T_B(36.5H) $\approx$ 270-280 K. The rain bands are also seen due to the higher T_B(36H) values against the background. They are clearly identified at all AMSR-E channels including low frequency ones. The areas of precipitation and heavy clouds prevent the estimation of wind speed. The corresponding areas are marked by a dark tone in Fig. 2b showing wind field derived from QuikSCAT SeaWinds data.

Figure 2. Envisat ASAR image with HH-polarization for 25 August 2004 at 01:52 UTC. Box is shown in higher resolution in Figure 4.
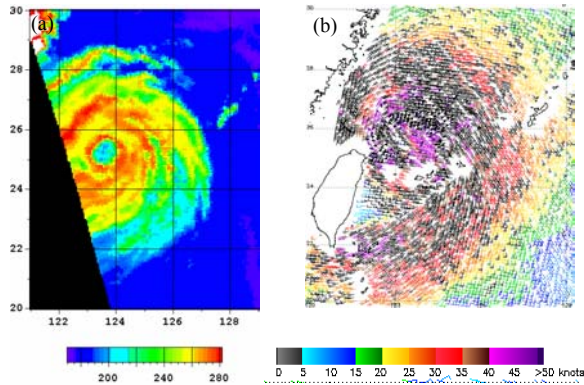

Figure 1. Brightness temperature at 36.5 GHz, H-polarization taken by Aqua AMSR-E at 4:40 UTC (a) and sea surface winds retrieved from QuikSCAT SeaWinds data taken at 09:32 UTC on 24 August 2004 (b).

Envisat ASAR image was taken on 25 August at 01:52 UTC when P_{min} = 963 mb, $W_{max} \approx$ 37 m/s and the Aere center was over the Taiwan Strait (Fig. 2). The Aere eye looks as a dark ellipsis the size of 40 x 30 km. It is surrounded by eye wall where maximum winds are observed. On ASAR image the eye wall represents a circle the width of about 40 km. The brightness of the circle is defined both wind speed and wind
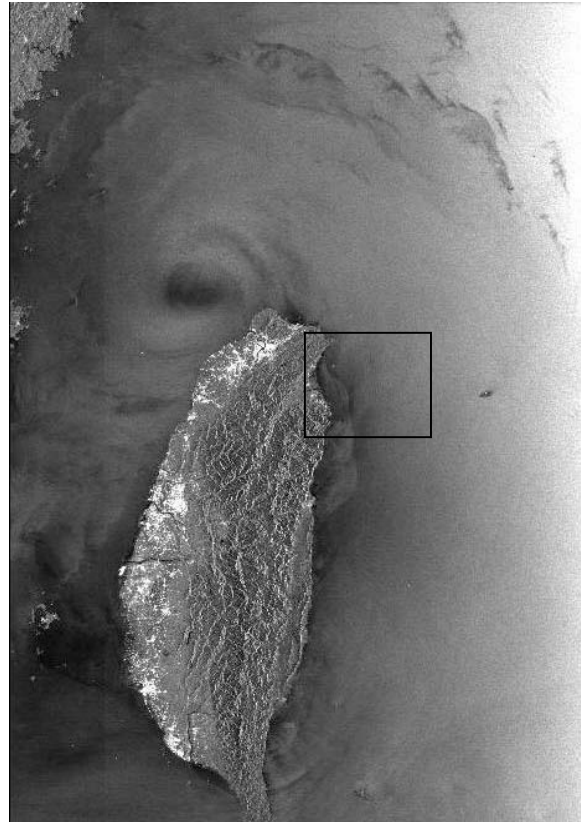
direction and reaches minimum/maximum when propagation direction of radar signal is crosswind/(upwind and downwind). Precipitation in the eye wall area as well as in the spiral rain bands are clearly identified on the image as the darker features. Distribution and phase state of precipitation within eye wall are inhomogeneous. Dark arc-like bands located closer to the external circle edge to the north and to the south of the typhoon center are very likely due to two way attenuation of radar signals in precipitation consisting in particular of hail. The most intensive precipitation is observed in a rain band to the north of the typhoon center. This band and the eye wall are characterized by the increased brightness temperatures at all AMSR-E channels except 89-GHz channels. The presence of hail and large rain droplets in these areas is confirmed by low T_B(89) values (Fig. 3). AMSR-E sensing was carried out in about 3 h after ASAR observations.

Alternating lighter and darker bands are distinguished on ASAR image to the east of central and northern Taiwan (Fig. 4). They are surface manifestations of the boundary layer rolls with the wavelength of 2-2.5 km. Their orientation corresponds to prevailing winds in the area. The large spatial extent of the rolls in TCs was revealed by RADARSAT-1 images of the Atlantic hurricanes (Katsaros et al, 2003). More frequent SAR observations will help to better understand their role in TC intensity change.
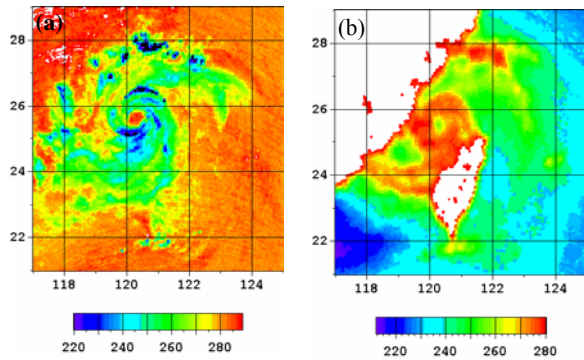
Figure 3. Brightness temperatures at 89 GHz, V-pol (a) and at 23.8 GHz, H-pol (b) taken by Aqua AMSR -E on 25 August 2004 at 05:20 UTC showing typhoon Aere structure.
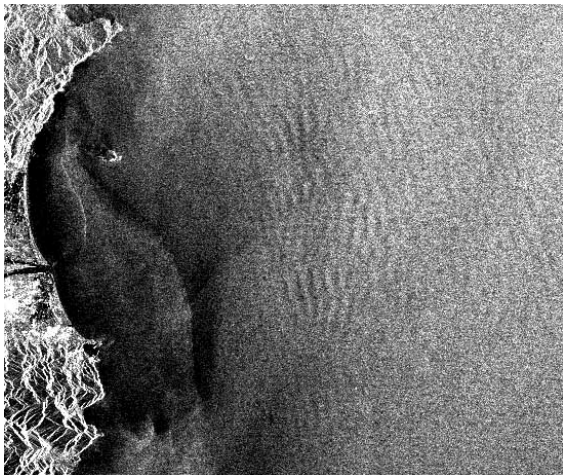

Figure 4. Surface manifestations of boundary layer rolls to the east of Taiwan on Envisat ASAR image taken on 25 August 2004. Note the striations across the image corresponding to the rolls. The striations have a wavelength of 2.0-2.5 km.

3.2 Typhoon Songda

Typhoon Songda formed on 27 August at 12:00 in the North Pacific near the Marshall Islands at 11.1°N, 167.0°E and reached typhoon strength on 29 August 2004. Two days later, Songda crossed over the Northern Mariana Islands and Guam. Maximum intensity was observed on 5 September at 09-12 UTC (P_{min} = 925 mb and W_{max} = 46 m/s) when Songda swept over Okinawa, bringing heavy rain and high winds. Typhoon reached a turning point of (28.9°N, 127.1°E) on 6 September at 03 UTC. Moving along the Japan coast of the Korean Strait it entered into the Japan Sea on 7 September with P_{min} = 945-950 mb. Songda was transformed into extratropical cyclone on 8 September at 06 UTC over the Sangar Strait.

Envisat ASAR images over Songda area were taken on 3, 4 and 6 September. The image for 3 September at 13:16 UTC crossed a western half of typhoon when P_{min} = 940 mb and W_{max} = 44 м/c. The radar backscatter variations result from strong winds and heavy precipitation. The gray-dark bands the width of 3-7 km surrounding the typhoon center and the

elongated dark patches at the bottom are due to attenuation of radar signals at two-fold propagation through rains and heavy clouds and due to modification of the small scale roughness caused by the droplet impacts with the sea surface (Fig. 5). Their relative contribution to the SAR signatures is a function of rain parameters, radar frequency, sensing geometry and calls for further investigation (Melsheimer, 2001; Katsaros et al, 2002; Mitnik et al., 2002; Vachon et al., 2001).
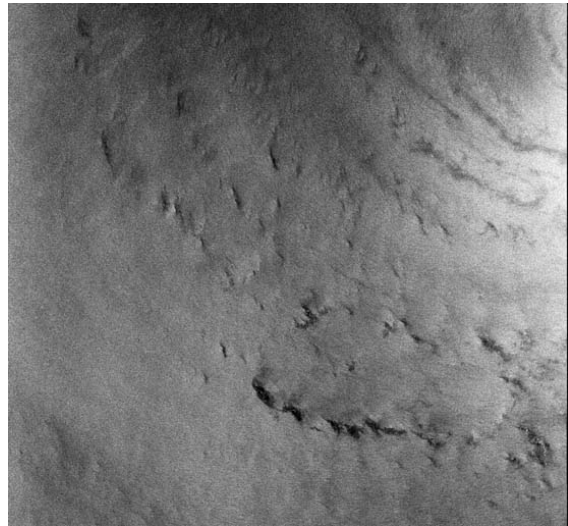

Figure 5. Envisat ASAR image taken on 3 September at 13:16 UTC showing the imprints of heavy precipitation in the left bottom quarter of typhoon Songda.

Strength of typhoon was not changed between 12 and 21 UTC on 3 September and its movement speed was 16-20 km/h. It permits to compare Envisat ASAR, Aqua AMSR-E and QuikSCAT SeaWinds data in spite of 4-h time difference between them. The spiral structure looks more clearly in fields of the AMSR-E T_Bs (Fig. 6a) as well as in fields of the total cloud liquid water content and total water vapor content retrieved from T_Bs values (Mitnik and Mitnik, 2003).
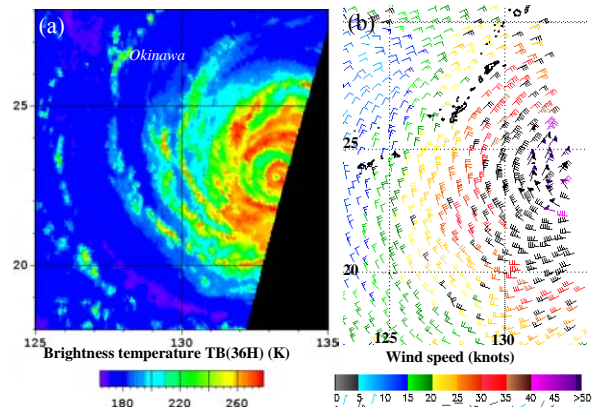

Figure 6. Brightness temperature at 36.5 GHz, H-polarization taken by Aqua AMSR-E at 4:40 UTC (a) and sea surface winds retrieved from QuikSCAT SeaWinds data taken at 09:32 UTC on 3 September 2004 (b).

Precipitation and heavy clouds are characterized by the highest $T_B^{V,H}$ values at frequencies $\nu \leq 37$ GHz and the eye wall and spiral rain bands stand up sharply against the background where Q-values are lower. Fine structure of precipitation is not detected due to antenna smoothing. High attenuation by rains and clouds at 13.4 GHz prevents the wind speed retrieval and the central area of Songda is marked by dark wind symbols (Fig. 6b).

According to AMeDAS data at Nago City, Okinawa for the 5th September, the change of pressure on the approaching of the center was steep, that indicated the eye was small and sharp. Next day the eye size was about 15 x 20 km (Fig. 7). Imprints of rain bands are clearly identified on the image.
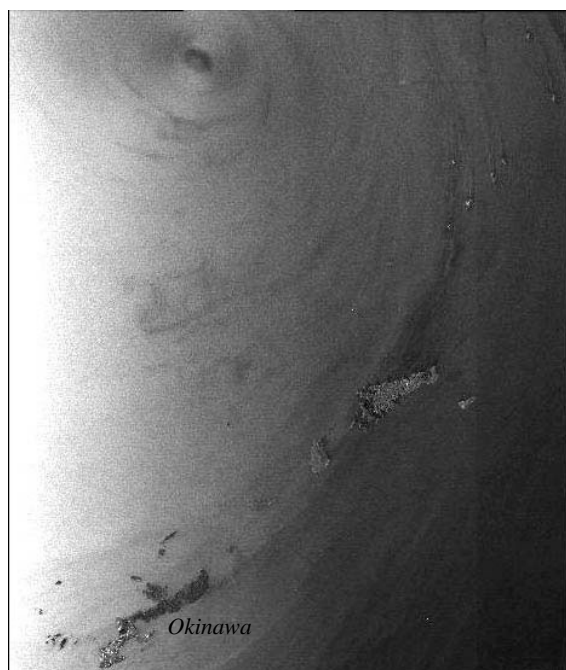

Okinawa

Figure 7. Envisat ASAR image of typhoon Songda taken on 6 September at 13:23 UTC.

4. CONCLUSIONS

TCs are easily detected with existing observations from polar and geostationary satellites in visible, infrared and microwave spectral bands. Spatial structure of typhoon in the microwave band is determined by distributions of precipitation, clouds, water vapor and surface wind. The passive microwave measurements at AMSR-E frequencies are more sensitive to precipitation and total cloud liquid water content as opposite to active microwave sensing at C-band (ASAR) and K-band (SeaWinds) where backscatter variations depend mainly on the wind speed and direction and precipitation. Correlation of atmospheric and ocean surface parameters manifests itself in correlation of the brightness temperatures $T_B^{V,H}(\nu)$ at different frequencies/polarizations as well as in correlation of $T_B^{V,H}(\nu)$ and the sigma-0 and gains an understanding of the TCs evolution. The interpretation of passive and active microwave data and the extraction of quantitative information on environmental parameters still require considerable expertise, experience and sophisticated tools.

6. REFERENCES

K.S. Friedman, and X. Li, "Monitoring hurricanes over the ocean with wide swath SAR", Johns Hopkins APL Technical Digest, vol. 21, p.p. 80-85, 2000.

K.B. Katsaros, P.W. Vachon, P.G. Black, P.P. Dodge, and E.W. Uhlhorn, "Wind fields from SAR: Could they improve our understanding of storm dynamics?", Johns Hopkins APL Technical Digest, vol. 21, p.p. 86–93, 2000.

K.B. Katsaros, P.W. Vachon, W.T. Liu, and P.G. Black, "Microwave remote sensing of tropical cyclones from space", J. Oceanography, vol. 58, p.p. 137-151, 2002.

A.I. Kalmykov, "Real-Aperture Radar (RAR) imaging from space," Radio Science Bulletin, N 276, p.p. 13-22, 1996.

C. Melsheimer, W. Alpers, and M. Gade, "Simultaneous observations of rain cells over the ocean by the synthetic aperture radar aboard the ERS satellites and by surface-based weather radars", J. Geophys. Res., vol. 106, N C3, p.p. 4665-4678, 2001.

L.M. Mitnik, G.I. Desyatova, and M.L. Mitnik, "The sea surface wind and cloudiness fields of tropical storm Agnes from data of satellite radiophysical sensing," Investigation of the Earth from Space (Soviet J. Remote Sensing), No. 6, p.p. 20-28, 1990 (in Russian).

M.L. Mitnik, L.M. Mitnik, and M.-K. Hsu, "Radar and microwave radiometer sensing of typhoon Ryan," Proc. IGARSS'97, Singapore, vol. 1, p.p.70-72, 1997.

L.M. Mitnik, M.-K. Hsu, and M.L. Mitnik, "Satellite active and passive microwave sensing of typhoon Angela", In: Remote Sensing of the Pacific Ocean by Satellites, R.A. Brown, ed., Earth Ocean & Space Publishing, p.p.78-89, 1998.

L. Mitnik, K-S. Chen, J.-T. Wang, M. Mitnik, and M.-K. Hsu, "Satellite microwave observations of typhoon Herb (1996) near Taiwan," The Global Atmosphere and Ocean System, vol. 8, N 1, p.p. 19-39, 2002.

L.M Mitnik, and M.L. Mitnik, "Retrieval of atmospheric and ocean surface parameters from ADEOS-II Advanced Microwave Scanning Radiometer (AMSR) data: Comparison of errors of global and regional algorithms," Radio Sciences, vol. 38, 8065, doi: 10.1029/2002RS002659, 2003.

C.L. Parkinson, "Aqua: An Earth-Observing satellite mission to examine water and other climate variables," IEEE Trans. Geosci. Remote Sensing, vol. 41, p.p. 173-183, 2003.

P.W. Vachon, P.G. Black, P.P. Dodge, K.B. Katsaros, P. Clemente-Colón, W. Pichel, and K. MacDonnell, "RADARSAT-1 Hurricane watch," Proc. IGARSS 2001, Sydney, Australia, p.p. 471-473, 2001.